Textures and Microstructures, 1991, Vols 14–18, pp. 829–834
Reprints available from the publisher
Photocopying permitted by license only

MICROSTRUCTURE AND MICROTEXTURE DEVELOPMENT DURING HIGH TEMPERATURE LOW CYCLE FATIGUE

S. Brodesser, S. Chen*, and G. Gottstein
Institut für Metallkunde und Metallphysik, RWTH Aachen, Kopernikusstr. 14, D - 5100 Aachen, FRG
* Los Alamos National Laboratory, Los Alamos, NM, USA

INTRODUCTION

During high temperature low cycle fatigue of metals microstructural changes take place due to the migration of grain boundaries, reorientation of grain boundaries with respect to the stress axis and - in materials with low stacking fault energy - dynamic recrystallization even at very small cyclic strain amplitudes. These phenomena have been reported in literature for a variety of materials [1,2], but there is still no satisfactory interpretation or predictive model for the observed complex microstructural changes. Recently, Watanabe et al. [2] determined by SACP the character of the grain boundaries in fatigued Al and concluded that ("special") grain boundaries with ordered structure (low Σ) would migrate not at all or less than less ordered ("general") boundaries. This conclusion, however, would not explain why grain boundaries orient themselves with regard to the stress axis and what final microstructure would be attained. The current contribution addresses these problems by an investigation into the orientation correlations and microtexture of high temperature fatigued Ni.

EXPERIMENTAL

The specimen consisted of high purity Ni (99.99%) which was deformed by tension/compression fatigue in high vacuum for 160 cycles at 600°C. The total (elastic and plastic) strain amplitude was 0.5% at a cyclic frequency of $13 \cdot 10^{-3}$Hz. Details of the experimental set-up, mechanical behavior and metallography are given elsewhere [3]. After the test a longitudinal section of the cylindrical specimen was prepared to reveal the microstructure in the interior of the gauge section of the specimen (Fig.1b). The orientation of the individual grains was determined from micro-Laue-patterns, obtained with synchrotron radiation according to a method introduced recently [4]. The beam size was about $5\mu m^2$, to ensure single grain illumination. The Laue patterns were recorded on a high speed X-ray film, digitized and evaluated by automatic pattern recognition [4]. The specimen was precisely translated under the beam according to the known microstructure in order to correlate grain orientation and topography, i.e. to determine next neighbor misorientation relationships.

RESULTS

In total 122 contiguous grains were evaluated yielding 271 orientation relationships between next neighbors. Fig.1b shows the microstructure of the analyzed specimen after the cyclic deformation. Comparing it to the initial microstructure (Fig.1a) one can recognize obvious microstructural changes like extensive grain growth and reorientation of grain boundaries with respect to the stress axis. For a more quantitative evaluation the grain sizes of the two specimens were measured before and after the deformation. The mean grain diameter after the deformation is 140 μm, i.e. about 15 times larger than the initial grain size of 9.5 μm. In both the initial and deformed microstructure there is a large difference between the minimum and the maximum grain size although for different reasons: Prior to deformation there is a relatively homogeneous grain size distribution, but the grains have different dimensions in the longitudinal and transverse direction. After cyclic deformation the differences in grain size are caused by some very large grains surrounded by much smaller grains.

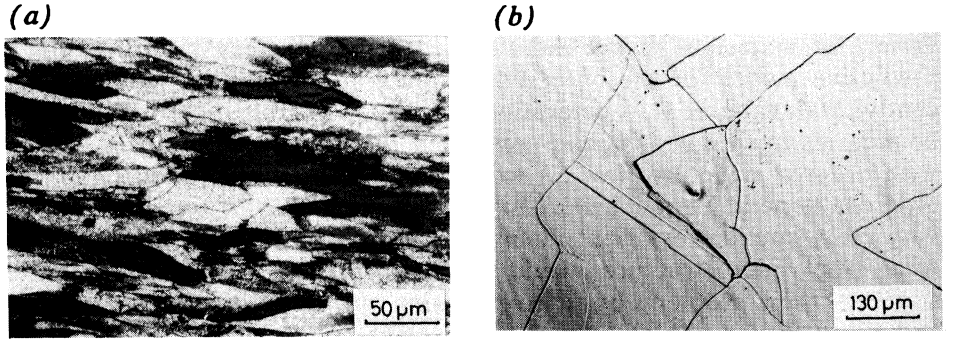

Figure 1a,b *Microstructure of (a) the specimen prior to deformation, mean grain radius R=9.5µm; (b) the cyclic deformed sample, mean grain radius R=140µm*

The undeformed specimen material was not randomly oriented, but revealed a strong fiber texture (Fig.2a) containing the {111} and the {100} fibers most likely due to prior extrusion processing of the material. The orientation distribution of the fatigued specimen (Fig.2b) is markedly different from the ODF of the undeformed material. The {100} fiber disappears and the original {111} fiber is decomposed into many discrete orientations. From the measured individual grain orientations an ODF was calculated by associating each orientation with an orientation distribution of Gauss-type scatter of 3°about the exact grain orientation (Fig.3). This calculated ODF is sufficiently similar to the ODF determined from pole figures, taking into account the small number of grains and the uncertainties introduced by ODF computation with truncated series expansion methods.

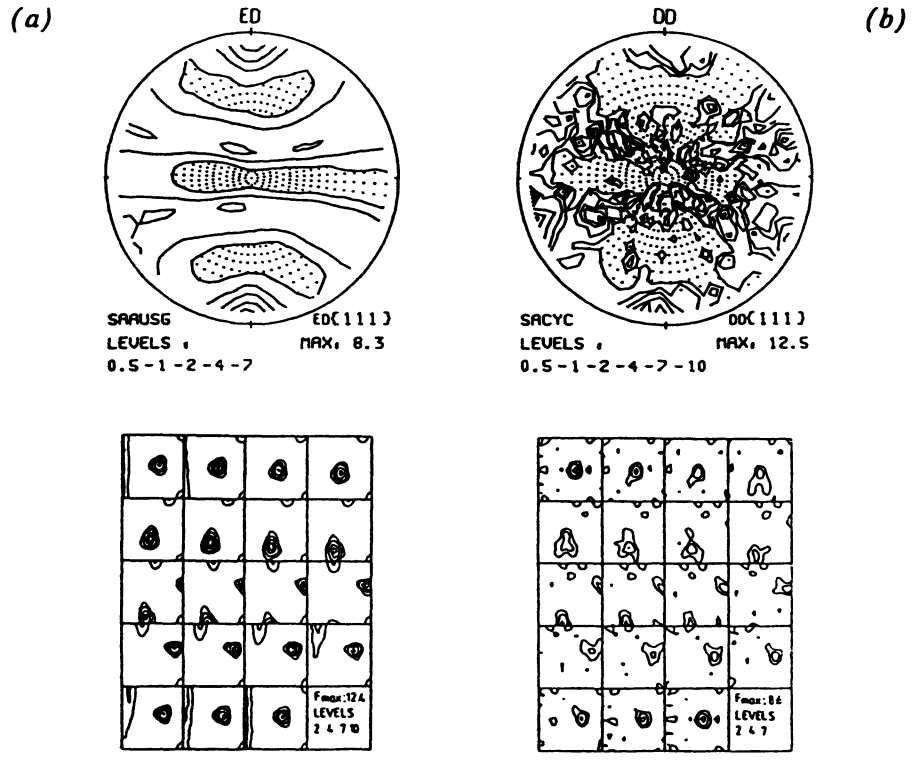

Figure 2 {111} pole figures and ODFs of the (a) original and (b) deformed material

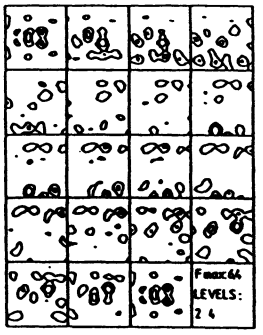

Figure 3 Gauss-ODF of the microtexture, calculated from the single orientations

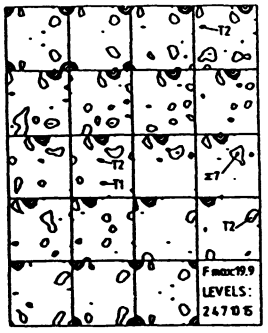

Figure 4 Gauss-MODF of the orientation relationships of neighboring grains

From the individual grain orientations the orientation relationship between next neighbour grains was calculated. From these data the misorientation distribution function (MODF) was determined by associating Gauss-type scatter with a spread of 3° to the exact orientation relationship.

It is presented in Euler space in Fig.4. Most conspicuous is the high orientation density around the origin (0°,0°,0°), i.e. the frequent occurrence (15%) of small angle boundaries. Another relative maximum of the MODF occurs at (57°,31°,57°) which corresponds to an orientation relationship of 38°<111>. Within a scatter of 10° this component accounts for 10% of all determined orientation relationships. The occurrence of particular orientation relationships was not found to be related to grain size.

To obtain information about the tendency to form "special" boundaries, we determined the frequency of CSL orientation relationships. Applying Brandon's criterion $\Delta\Theta=15°/\sqrt{\Sigma}$ with $\Delta\Theta$ the permissible misorientation from the exact CSL orientation relationship and Σ the reciprocal density of coincidence sites [5], the frequency distribution for $3\leq\Sigma\leq99$ shown in Fig.5 is obtained. We notice a large fraction of $\Sigma\leq15$ boundaries with maxima at $\Sigma3$ and $\Sigma9$, i.e. twins of first and second order. But there is also noticeable occurrence of $\Sigma11$, 13, 15 and even 45 and 67. Remarkably low is the frequency of $\Sigma5$ and $\Sigma7$ boundaries. The latter seems contradictory to the result that the MODF has a maximum at 38°<111> while $\Sigma7$ corresponds to a misorientation of 38.2°<111>. The discrepancy is due to the fact that most of the orientations which contribute to the MODF peaks at 38°<111> have an orientation difference of more than $15/\sqrt{7}=5.7°$ from the ideal $\Sigma7$ orientation relationship. If $\Delta\Theta$ would be increased to 10°, about 26% of the special boundaries would be $\Sigma7$ boundaries. The occurrence is obviously coupled with grain size. Virtually no low Σ boundary was found between large grains, but many low Σ boundaries existed between small grains.

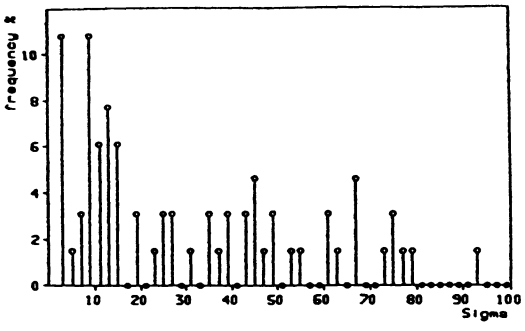

Figure 5
Frequency of low Σ-boundaries after cyclic deformation except Σ=1. As a result of the limited number of grains one single Σ-boundary corresponds to 1.5%

DISCUSSION

A conspicuous result is the frequent occurrence of <111> rotations, which leads to a maximum of the MODF at 38°<111> (Fig.4). These <111> orientation relationships between next neighbour grains cannot be attributed to remnants of the original <111> fiber components, since the majority of the orientations after deformation do not belong to fiber components. This becomes evident from Fig.6 where the inverse pole figure of the stress axis is plotted as computed from the individual grain orientations. We surmise

that this reorientation is forced by the deformation process and propose the following interpretation. Because of the very small strain amplitudes, the compatibility at the grain boundaries is considered of less importance so that each crystal can essentially deform independently. For single crystal deformation in tension/compression the stable orientations are the corner orientations and the zone that contains the glide plane normal and the slip direction. Any orientation will therefore move toward this zone, except for the exact corner orientations. The orientation groups identified in the inverse pole figure can be related to this process. The orientations in regions close to the <001> and <111> corners are probably remnants of the initial fiber orientations, which have not reoriented very far owing to their proximity to the exact corner orientations. The two groups in the center are the cluster of orientations moving toward the [12$\bar{1}$] zone.

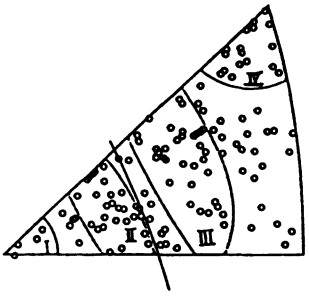

Figure 6 Inverse pole figure of the stress-axis of the single orientations

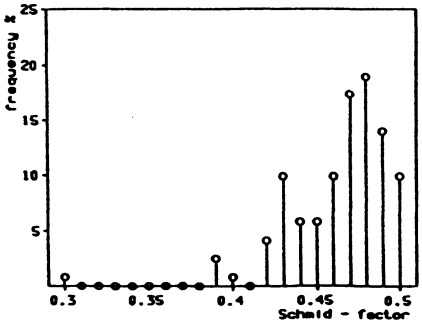

Figure 7 Frequency distribution of the Schmid-factors after cyclic deformation

This interpretation is supported by two other observations. The [12$\bar{1}$] zone comprises orientations of high Schmid factors μ, the average being μ=0.486. The distribution of Schmid factors as calculated from the measured individual orientations by assuming single slip deformation (Fig.7) actually reveals the highest maximum at 0.48, with an average of 0.46. The small peak at small μ is probably due to the group of corner orientations. A Schmid factor so close to 0.5 as measured requires the angle between slip plane normal and stress axis to be close to 45°, i.e. in the pertaining crystal there is a {111} plane close to 45° to the stress axis. With the {111} planes closely aligned, the orientation relationship between such grains will be close to a <111> rotation, which is thus found quite often and produces the MODF maximum at a 38°<111> orientation relationship. The proposed model does not provide readily an explanation for the observed grain boundary reorientation under 45° to the applied stress and there may be more than one reason. Within the proposed model there is also the possibility that the anisotropy of grain boundary mobility contributed to the observed grain boundary alignment. With the majority of orientation relationship being <111> rotations and the <111> axis being oriented under 45° with respect to

the stress axis, the grain boundary under 45° is a pure twist boundary. The mobility of {111} boundaries is known to be very low [6]. Correspondingly the grains should exhibit long twist boundary segments under 45° to the stress axis as observed. Further investigations are definitely necessary to clarify this problem.

CONCLUSIONS

(1) The microtexture evolution during high temperature low cycle fatigue of Ni was investigated by orientation mapping with synchrotron radiation.

(2) Substantial texture changes were observed during deformation which are associated with grain growth, grain boundary reorientation and dynamic recrystallization.

(3) The misorientation distribution function reveals conspicuous frequency of small angle grain boundaries and <111> rotations. Correspondingly the low Σ boundaries consisted of small angle boundaries and <111> rotations, but also twin chains.

(4) It is proposed to attribute the orientation changes to unconstrained deformation of grains under cyclic tension/compression deformation. This interpretation is supported by the finding that the average Schmid factor increases strongly during deformation and that the glide planes tend to arrange under 45° to the stress axis.

REFERENCES

1 S. Chen and G. Gottstein, *Acta metall.* **36**, 3093 (1988)
2 V. Raman, T. Watanabe, and T.G. Langdon, *Acta metall.* **37**, 705 (1989)
3 S. Chen, Ph.D. Dissertation, Michigan State University, 1989
4 G. Gottstein, Proc. ICOTOM 8, (1988) p.195
5 D.G. Brandon; *Acta metall.* **14**, 1479 (1966)
6 G. Gottstein, H.C. Murmann, G. Renner, C. Simpson, and K. Lücke, *Textures of Materials*, Springer-Verlag, Berlin (1978) p.521

ACKNOWLEDGEMENT

The support of the Department of Energy, Office of Basic Energy Sciences, under grant DE-FG02-85ER 45205 is gratefully acknowledged. Part of the research was conducted at the National Synchrotron Light Source, Brookhaven National Laboratory. The authors are very much indebted to Dr. D. Cox for setting up the beam line.